Brick masonry infills in seismic design of RC frame buildings: Part 2 – Behaviour

Diptesh Das and C.V.R. Murty

Non-linear pushover analysis was performed on five RC frame buildings with brick masonry infills, designed for the same seismic hazard as per Eurocode, Nepal Building Code and Indian and the equivalent braced frame methods given in literature. Infills are found to increase the strength and stiffness of the structure, and reduce the drift capacity and structural damage. The plinth beam is significant when infills are considered in the modelling. Infills reduce the overall structure ductility, but increase the overall strength. Building designed by the equivalent braced frame method showed better overall performance.

A method based on the equivalent diagonal strut approach for analysis and design of infilled frames subjected to in-plane forces was proposed in literature[1]. The method accounts for inelastic and plastic behaviour of infilled frames considering the limited ductility of infilled materials. It provides a rational basis for estimating the lateral strength and stiffness of the infilled frames as well as the infill diagonal cracking load. Also, an analytical macro-model was proposed based on equivalent strut approach, integrated with a smooth hysteretic model for representing masonry infills in nonlinear analyses (for example, monotonic pushover analysis or time history analysis)[2]. The hysteresis model included stiffness degradation, strength determination and slip, to replicate a wide range of hysteretic force-displacement behaviour resulting from different designs and geometries. The envelope properties of the strut, namely the stiffness and the control points of the force-deformation relations, *Fig* 1, were determined from mechanics of infill-frame interaction proposed earlier[1]. The monotonic lateral force-deformation relationship is a bilinear curve with an initial elastic stiffness till the yield force, V_y, and there on a post-yield degraded stiffness until the maximum force, V_m. The maximum lateral

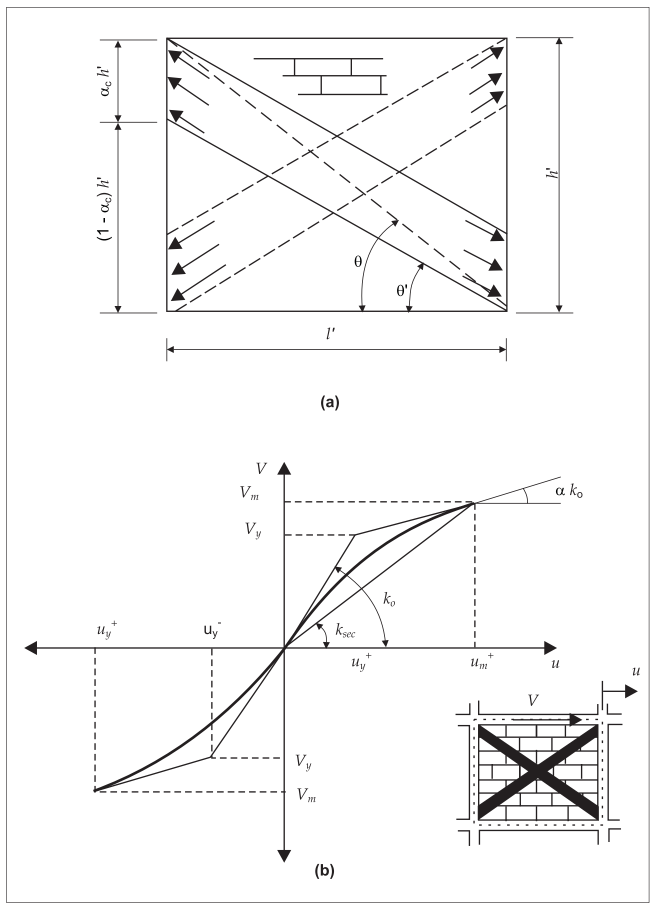

Fig 1 Equivalent strut idealisation of a masonry infill panel used in the macro-model of infills: *(a)* Definition of diagonal strut in infill, and *(b)* Strength envelope for masonry infill panel[1].

force , V_m , and the corresponding displacement, u_m , in the infill masonry panel were calculated as:

$$V_m \leq \begin{cases} A_d f_m' \cos\theta \\ \dfrac{\tau_s t l'}{(1-0.45\tan\theta')} \text{ and} \\ 1.25(MPa)tl' \\ \dfrac{\varepsilon_m' L_d}{\cos\theta} \end{cases} \quad ...(1)$$

$$u_m = \frac{\varepsilon_m' L_d}{\cos\theta} \quad ...(2)$$

where,

t = the thickness or out-of-plane dimension of the infill panel

θ = $\tan^{-1}(h/l)$

f_m' = masonry prism strength

ε_m' = corresponding strain

τ_s = shear strength or cohesion of masonry.

The area, A_d , and the length, L_d , of the equivalent diagonal strut were obtained from:

$$A_d = \frac{(1-\alpha_c)\alpha_c t h' \dfrac{\sigma_c}{f_c} + \alpha_b t l' \dfrac{\tau_b}{f_c}}{\cos\theta} \leq \frac{0.5 t h' \dfrac{f_a}{f_c}}{\cos\theta} \quad ...(3)$$

$$L_d = \sqrt{(1-\alpha_c)^2 h'^2 + l'^2} \;, \quad ...(4)$$

where the quantities α_c, α_b, σ_c, τ_b, f_a and f_c depend on the geometric and material properties of the frame and the infill panel. These quantities are calculated as mentioned below.

The upper bound or failure normal contact stresses, σ_{c0} and σ_{b0} , at the column-infill interface and beam-infill interface respectively were calculated as:

$$\sigma_{c0} = \frac{f_c}{\sqrt{1+3\mu_f^2 r^4}} \quad ...(5)$$

$$\sigma_{b0} = \frac{f_c}{\sqrt{1+3\mu_f^2}} \quad ...(6)$$

where,

r = the aspect ratio of the infill (=h/l, where $h<l$),

f_c = the compressive strength of the masonry

μ_f = the coefficient of friction of the frame-infill surface.

The centre-line dimensions of the height and the length of the infill are denoted by h and l respectively. The contact lengths $\alpha_c h$ and $\alpha_b l$ at the column-infill and beam-infill interfaces respectively were expressed as

$$\alpha_c h = \sqrt{\frac{2M_{pj} + 2\beta_0 M_{pc}}{\sigma_{c0} t}} \leq 0.4h' \quad ...(7)$$

$$\alpha_b l = \sqrt{\frac{2M_{pj} + 2\beta_0 M_{pb}}{\sigma_{b0} t}} \leq 0.4l' \quad ...(8)$$

where,

M_{pj} , M_{pc} and M_{pb} are the plastic moment capacities of the joint, column and beam, respectively;

h' = height

l' = length of the infill panel.

The recommended value of β_0 to be used in the model was 0.2.

The compressive stress, f_a , of infill in its central region was given by:

$$f_a = f_c\left[1-\left(\frac{L_d}{40t}\right)^2\right] \quad ...(9)$$

The actual normal contact stresses, σ_c and σ_b , are calculated using:

$$\left.\begin{aligned} \sigma_c &= \sigma_{c0}\left(\frac{A_b}{A_c}\right) \\ \sigma_b &= \sigma_{b0} \end{aligned}\right\} \text{ if } A_b \leq A_c \quad ...(10)$$

$$\left.\begin{aligned} \sigma_b &= \sigma_{b0}\left(\frac{A_c}{A_b}\right) \\ \sigma_c &= \sigma_{c0} \end{aligned}\right\} \text{ if } A_b > A_c \quad ...(11)$$

where,

$$A_c = r^2 \sigma_{c0} \alpha_c (1-\alpha_c-\mu_f r)$$

$$A_b = \sigma_{b0} \alpha_b (1-\alpha_b-\mu_f r)$$

The contact shear stresses, τ_c and τ_b , at the column-infill interface and the beam-infill interface respectively were given as:

$$\tau_b = \mu_f r^2 \sigma_c \quad ...(12)$$

$$\tau_c = \mu_f \sigma_b \quad ...(13)$$

The angle, θ', of masonry diagonal strut at shear failure was obtained from the relation:

$$\theta' = \tan^{-1}[(1-\alpha_c)h'/l'] \quad ...(14)$$

The monotonic lateral force-displacement curve was completely defined by the maximum force, V_m, the corresponding displacement, u_m, the initial stiffness, K_0, and the ratio α of the post-yield to initial stiffness. The initial stiffness, K_0, of the infill masonry panel was given by:

$$K_0 = 2\left(\frac{V_m}{u_m}\right) \quad ...(15)$$

The lateral yield force, V_y, and the displacement, u_y, of the infill panel was calculated from the geometry of the curve as follows:

$$V_y = \frac{V_m - \alpha K_0 u_m}{(1-\alpha)} \quad ...(16)$$

$$u_y = \frac{V_m - \alpha K_0 u_m}{K_0(1-\alpha)} \quad ...(17)$$

A value of 0.1 for the ratio, α, was recommended in the model.

Pushover analysis

Displacement-controlled pushover analysis is performed of example three-dimensional symmetric buildings using the computer program *SAP2000*[3]. Details of these buildings have been discussed already in the companion paper[4]. At each floor level, the pushover force is applied at the point of design eccentricity, that is, $0.05b_i$ from the plan centroid as given in IS 1893, where b_i is the floor plan dimension of floor i perpendicular to the direction of force. The rigid diaphragm action of the floor slabs is considered. The proportion of floor lateral loads is taken to be the first lateral mode shape (for shaking in the direction of pushover), which is obtained for the free vibration analysis of the building models. This is prescribed to be generally valid for buildings with fundamental periods of vibration up to about 1.0 s. The first mode pushover force, f_{1i}, at floor i is calculated as

$$f_{1i} = \lambda \phi_{1i} W_i \quad ...(18)$$

where,

ϕ_{1i} = mode shape coefficient in mode 1 at floor i

W_i = seismic weight of floor i

λ = scalar multiplier depending on the pushover displacement.

A target displacement of $0.04H$ is specified as the limit for the roof displacement, where H is the height of the building.

The capacity spectrum ordinates, namely spectral acceleration, S_a, and spectral displacement, S_d, are obtained from the capacity curve with the help of the following relations[5]:

$$S_a = \frac{V/W}{\alpha_1} \quad ...(19)$$

$$S_d = \frac{\Delta_{roof}}{PF_1 \phi_{roof,1}} \quad ...(20)$$

In equations (19) and (20),

$$PF_1 = \left[\frac{\sum_{i=1}^{N}(w_i\phi_{i1})/g}{\sum_{i=1}^{N}(w_i\phi_{i1}^2)/g}\right] \quad ...(21)$$

$$\alpha_1 = \frac{\left[\sum_{i=1}^{N}(w_i\phi_{i1})/g\right]^2}{\left[\sum_{j=1}^{N}w_j/g\right]\left[\sum_{k=1}^{N}(w_k\phi_{k1}^2)/g\right]} \quad ...(22)$$

where,

PF_1 = modal participation factor of the first natural mode

α_1 = modal mass coefficient of the first mode

w_i/g = mass of the building at level i;

ϕ_{i1} = mode shape coefficient of mode 1 at level i

N = uppermost level in the structure

N = base shear from pushover analysis

W = the seismic weight taken as dead weight plus part live loads

Δ_{roof} = roof displacement from pushover analysis.

Modelling of plastic hinges

RCC frame members

Plastic hinge length

The plastic hinges in members are assumed to form at a distance equal to half the average plastic hinge length, l_p, where l_p is given by Baker's formula[6]:

$$l_p = 0.8k_1k_3\left(\frac{z}{d}\right)c \quad ...(23)$$

where,

z = distance of critical section to the point of contraflexure

d = effective depth of the member

c = neutral axis depth at ultimate moment

k_1 = 0.7 (for mild steel)

k_1 = 0.9 for cold-worked steel

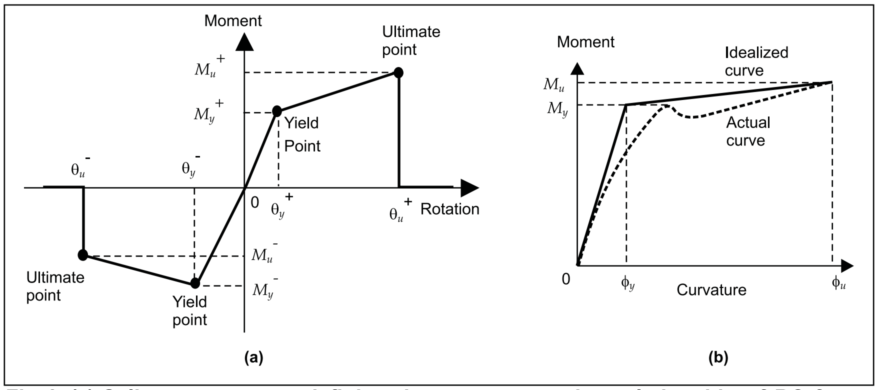

Fig 2 ***(a)*** **Salient parameters defining the moment-rotation relationship of RC frame members for use in the pushover analysis; and** ***(b)*** **Idealisation of moment-curvature relationship for RC frame members**

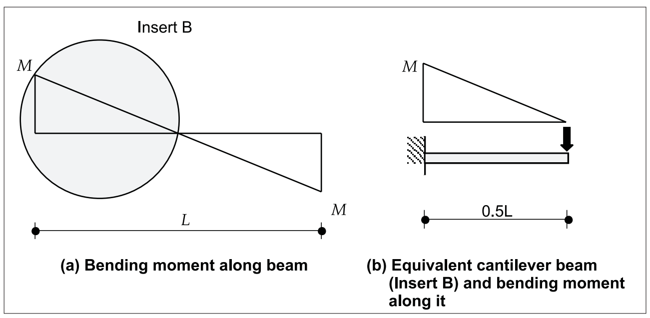

Fig 3 Equivalent cantilever beam idealisation to obtain moment-rotations from moment curvature relations

$$k_3 = \begin{cases} 0.6 & f_c^{'} \geq 35.2\ MPa \\ 0.6 + 0.0128(f_c^{'} - 11.7) & 35.2\ MPa < f_c^{'} < 11.7\ MPa \\ 0.9 & f_c^{'} \leq 11.7\ MPa \end{cases} \qquad ...(24)$$

where,

$f_c^{'}$ = 0.8 times the cube strength.

The plastic hinges are modelled by the moment-rotation relationships shown in *Fig* 2*(a)*. The yield and the ultimate points may be different in sagging and in hogging. For the plastic hinges in columns, axial force, P, versus bending moment, M, interaction is also included. Plastic hinges associated with the axial force, P, versus axial deformation , v, relationships of brick masonry panels, are allowed to form in middle of the strut members.

Moment-rotation relationships

The moment-curvature $(M - \phi)$ curves of columns are calculated for axial load corresponding to full *DL* and 25 percent *LL*, using the computer program PM_INT[7]. These curves are idealised as bilinear curves using initial tangent and ultimate moment, *Fig* 2*(b)*.

The bending moment diagram of a member under lateral forces varies linearly. The moment-rotation ($M - \theta$) relationship for this distribution of moments is obtained using the $M - \phi$ relationship. A fixed-end member can be replaced by an equivalent cantilever member of half span, with a concentrated load at its tip, *Fig* 3, if the point of contraflexure is at the midspan. The yield and ultimate rotations θ_y and θ_u respectively, are obtained by the following relations:

$$\theta_y = \frac{M_y\left(\frac{L}{2}\right)}{4EI} \qquad ...(25)$$

$$\theta_u = \theta_y + l_p(\phi_u - \phi_y) \qquad ...(26)$$

where,

L, E, and I = length, modulus of elasticity and moment of inertia of the member respectively

ϕ_u and ϕ_y = idealised ultimate and yield curvatures of the section, respectively

l_p = length of the plastic hinge given by equation (23).

The same computer program is used to obtain the $P - M$ interaction curves for columns. These are idealised by multi-linear curves as shown in *Fig* 4*(a)*.

Infill wall panels

Axial load-deflection relationships

The contribution of masonry infill panels to the response of infilled frame is modelled by replacing the infill panels with equivalent diagonal struts. The lateral force-deformation relationship of these struts, *Fig* 4*(b)* is obtained using relations

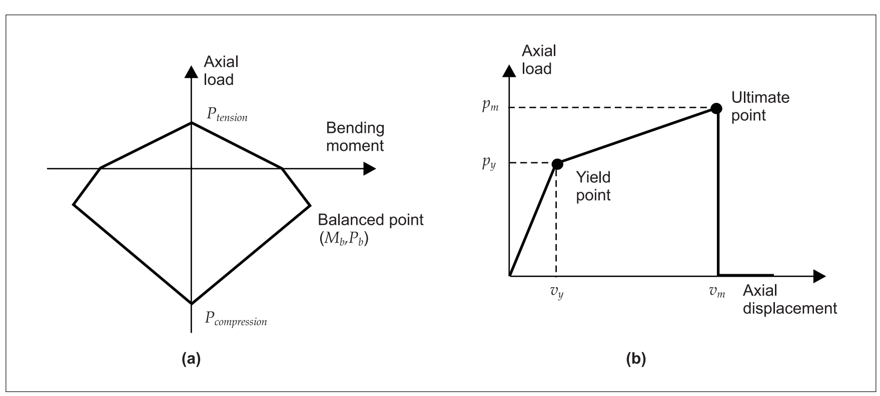

Fig 4 ***(a)*** **Idealised P-M interaction diagram for the column members; and** ***(b)*** **Axial load displacement curve for equivalent diagonal strut**

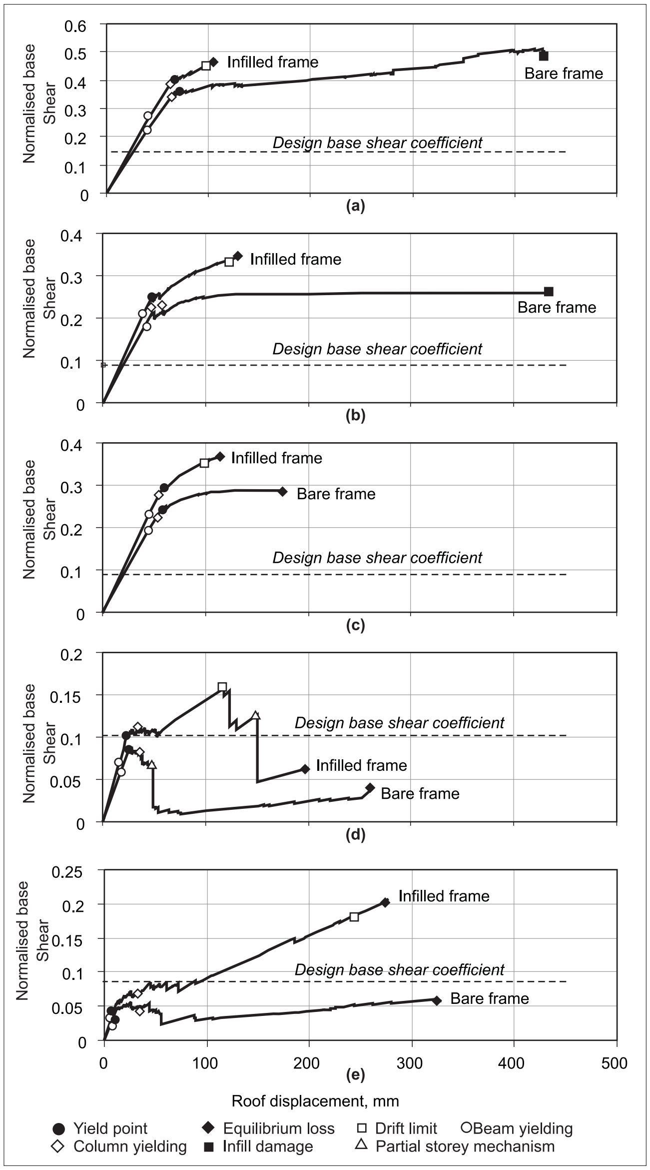

Fig 5 Capacity curves of buildings designed by *(a)* IS:456, *(b)* IS:13920, *(c)* EC8, *(d)* NBC201 and *(e)* EBF method

given in literature[2]. In these expressions, $f_m^{'}$ is taken as 4.0 MPa and $\varepsilon_m^{'}$ as 0.00007 from the results of brick prism tests reported in literature[8]. The shear strength of masonry is taken as 2.5 times the permissible shear stress value given by IS 1905 : 1987 and the coefficient of friction μ_f as 0.45[9,1,10].

Assuming small deformation, the idealised yield force, P_y, and idealised maximum force, P_m, in the axial direction and the corresponding displacements, namely v_y and v_m, are obtained from the corresponding quantities in the lateral direction obtained from equations (1) to (17):

$$P_m = \frac{V_m}{\cos\theta},$$

$$v_m = u_m \cos\theta$$

$$P_y = \frac{V_y}{\cos\theta} \qquad ...(27)$$

$$v_y = u_y \cos\theta$$

...(27)

Results and discussions

The normalised base shear-roof displacement curves of all the buildings, which are modelled by the design philosophies of IS 456, IS 13920, EC8, NBC201 and EBF method respectively, are shown in *Fig* 5. The capacity spectra of the buildings are compared in *Fig* 6. The important response parameters and the details of plastic hinges formed are shown in *Tables* 1, 2 and 3, respectively.

Due to the presence of infill walls, there is a reduction in the displacement of the structure[11]. This drop in the ultimate spectral displacement is high in case of IS 456 and IS 13920 designs, namely by 77 percent and 72 percent respectively. The decrease in displacement in case of EC8 and NBC201 buildings are in the intermediate range (that is, by 38 percent and 21 percent respectively), while it is least in EBF building (14 percent). The ratio of the ultimate displacement (obtained from the capacity curve) and the ultimate spectral displacement (obtained from the capacity spectrum) Δ_{roof} / S_{du} is lowest for the infilled frame designed as per EBF method. This indicates that the effect of first mode on the response is the maximum for this building.

The stiffness values and stiffness ratios for different buildings are given in *Table* 1. The infills result in an increase

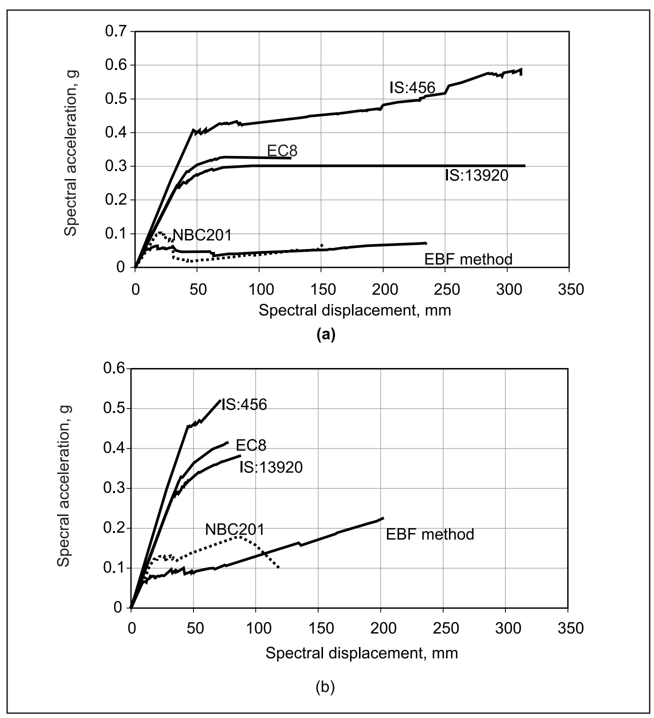

Fig 6 Capacity spectra of buildings designed by different procedures: *(a)* Bare frame, and *(b)* Infilled frame

Table 1: Measured response parameters obtained in buildings designed by different design procedures

Response Parameters	*Design procedure*									
	IS 456		*IS 13920*		*EC8*		*NBC201*		*EBF Method*	
	Bare	*Infilled*	*Bare*	*Infilled*	*Bare*	*Infilled*	*Bare*	*Infilled*	*Bare*	*Infilled*
S_{dy}, mm	47	46	34	34	42	40	18	19	11	11
S_{du}, mm	311	72	315	88	126	78	152	120	235	202
$S_{du,\,B}$ /$S_{du,I}$	4.32		3.58		1.62		1.27		1.16	
Δ_{roof} /S_{du}	1.39	1.5	1.37	1.5	1.4	1.5	1.72	1.68	1.4	1.37
Yield drift, percent	0.46	0.43	0.31	0.31	0.39	0.37	0.17	0.18	0.10	0.10
Ultimate drift, percent	2.88	0.67	2.92	0.81	1.17	0.72	1.41	1.11	2.18	1.87
Initial stiffness, kN/m	80100	92179	63190	74463	64080	75353	49292	61558	67582	79456
Initial stiffness ratio (Infilled/bare)	1.15		1.18		1.18		1.25		1.18	
$S_{a,\,yield}$, g	0.41	0.45	0.24	0.29	0.28	0.33	0.10	0.13	0.06	0.07
$S_{a,\,ultimate}$, g	0.59	0.52	0.30	0.38	0.32	0.42	0.10	0.18	0.07	0.23
Design base shear, kN	1335	1335	801	801	828*	828*	921^{+}	921^{+}	996	996
Yield base shear, kN	3622	4023	2163	2537	2492	2937	890	1113	609	742
Ultimate base shear, kN	5215	4637	2697	3400	2848	3738	908	1593	797	2502
Ultimate strength ratio (infilled/bare)	0.89		1.26		1.31		1.75		3.14	
Design base shear coefficient	0.150	0.150	0.090	0.090	0.093*	0.093*	0.104 $^{+}$	0.104 $^{+}$	0.090	0.090

** Modified by multiplying with the ratio of ordinates of design spectrum; + Combined value*

in the stiffness of structures. Stiffness increments in all the buildings, however, are more or less the same, with the provisions of NBC resulting in the largest stiffness increase (that is, 25 percent). The increase in initial stiffness is, however, far less than what is expected, that is, about 3.8 times higher than that of the bare frame, as seen in literature[12]. The unreinforced brick masonry considered in the present study is relatively weak in strength. Since the model used to obtain the stiffness of the infill strut uses this strength, the stiffness of the infilled frames is only marginally enhanced by the infill masonry. Moreover, the equivalent strut model of the infill panel used in the present study prescribes only cross sectional area of the strut, based on which load-deformation relationships are subsequently developed. Different section properties like sectional area, moment of inertia and shear area, are required to be separately provided in the computer program as input. The program is sensitive to all these section properties. The cross-sectional area, which is the only section property known, is provided as input and this resulted in a less stiff strut member. Consequently, during the pushover analysis, when the infill panels were simulated by these strut members, they contributed to a lesser extent than expected to the overall response of the structure. Also, the minimum of the plastic moment capacities of the two adjoining columns and the two adjoining beams has been used to obtain strut properties. The strut elements are less stiff for all these reasons. The behaviour of the RC frame thus dominated the overall response of the building.

Table 1 shows the ultimate strength values and their ratios for the different buildings studied. The infill walls act as lateral load resisting structural elements and result in an increase in the strength of the buildings. The strength increments for IS 13920 and EC8 design are low. A comparatively larger increment of 75 percent takes place in case of the NBC201 building, whereas a substantial increase of 214 percent is observed in the building designed by EBF method. Against these, an 11 percent decrease in strength is found in the IS 456 building due to early failure of the infilled structure. This implies that the inherent strength of the masonry infill walls is most effectively utilised in the design philosophy of EBF method.

One significant influence of infill walls on the response of the building is the reduction in the value of ductility factor, μ, as is evident from the μ values given in *Table* 2. The decrease is because the ultimate drift of the building with infill walls is lower than that of the bare frame, while their yield displacements are more or less the same, *Fig* 7. The reductions are high for the buildings designed by IS 456 and IS 13920 but

Table 2: Derived response parameters obtained in buildings designed by different design procedures

Response parameters	*Design procedure*									
	IS 456		*IS 13920*		*EC8*		*NBC201*		*EBF Method*	
	Bare	*Infilled*	*Bare*	*Infilled*	*Bare*	*Infilled*	*Bare*	*Infilled*	*Bare*	*Infilled*
Ductility factor, μ	6.62	1.57	9.26	2.59	3.00	1.95	8.44	6.32	21.36	18.36
Overstrength ratio, Ω_0	2.71	3.01	2.70	3.17	3.01	3.55	0.97	1.21	0.61	0.75
Redundancy ratio, Ω_r	1.44	1.15	1.25	1.34	1.14	1.27	1.02	1.43	1.31	3.37
Overstrength factor, Ω	3.91	3.47	3.37	4.24	3.44	4.51	0.99	1.73	0.88	2.51
Response reduction factor, *R*	25.9	5.1	31.2	8.7	10.3	7.7	8.4	5.9	17.1	15.0

Table 3: Distribution of damage (number of members yielding) in buildings designed by different design procedures

Members	Design procedure									
	IS:456		IS:13920		EC8		NBC201		EBF method	
	Bare	Infilled	Bare	Infilled	Bare	Infilled	Bare	Infilled	Bare	Infilled
Columns	98	41	97	53	86	81	54	73	68	71
Beams	144	44	122	118	97	92	46	76	121	127
Infill walls	-	5	-	6	-	3	-	13	-	6

are significantly lower for the buildings designed by NBC 201 and EBF methods. Therefore, even if the ductility value is estimated on the basis of the bare structure only, the error of overestimating μ is minimum in case of EBF method of design.

Due to the presence of infills, there is an increase in the value of overstrength factor, Ω. This increase may be attributed to the higher ultimate spectral displacement, $S_{a,ultimate}$, of the stiffer infilled structure. The increase is maximum in case of EBF method (210 percent); it is also high, compared to the remaining, for NBC201 (75 percent). The largest reserve strength due to the presence of the infills is therefore mobilised in the NBC building during earthquake shaking.

Since natural period and μ of the infilled frame are lower than those of the bare frame, the ductility reduction factor, $R\mu$, is also lower for the infilled frame. Although Ω values for the infilled frames are higher, this increase is comparatively lower than the decrease in $R\mu$. Consequently, there is a decrease in response reduction factor due to presence of infills. The decrease for the building designed by EBF method (13 percent) is comparatively lower than those in case of the other buildings (80 percent, 72 percent, 25 percent and 30 percent).

When the behaviour of the buildings designed by different methods are compared, it is observed that the building designed by EBF method has the maximum ability to sustain deformation during earthquake shaking. The deformations of the buildings designed as per IS 456, IS 13920 and EC8 are much lower.

From the stiffness values given in *Table* 1, it is observed that IS 456 design resulted in the stiffest structure and NBC 201 design the most flexible one. Buildings designed by IS 13920, EC8 and EBF method have same stiffness values in the intermediate range. The ultimate strength of the building designed by IS 456 is the maximum and those designed by NBC and EBF method are in the lowest range.

High value of ductility factor, μ, namely 18.36 is observed for the infilled structure that is designed following EBF method and hence, a more desirable and ductile response is expected from this building. The high value of ductility for this building may be attributed to its early yielding. Ductility values for all the other buildings are much lower.

From the values given in *Table* 1, it is evident that the overstrength factor, Ω, for the first three infilled frame buildings are higher than those for the NBC and the EBF buildings. The reserve strengths against lateral earthquake loading in the latter two buildings are therefore lower. This is due to the fact that in the definition of Ω, the redundancy is also included. In NBC and EBF method designs, the infill walls are modelled and are then included in the analyses also. This reduced the redundancy inherent in the structural system and Ω values for these buildings subsequently reduced. In these buildings, design lateral forces are shared partially by the infill struts and partially by the bare frame members. Therefore, when only the bare frames are considered, Ω equal to or slightly less than 1.0 are obtained. The 1997 Uniform Building Code recommends an overstrength value of 2.8[13] for moment resisting frame systems. Of all the different buildings, the Ω value of 2.51 corresponding to the infilled frame building designed by EBF method is closest to Ω prescribed by UBC97. For the other buildings, it is more. In

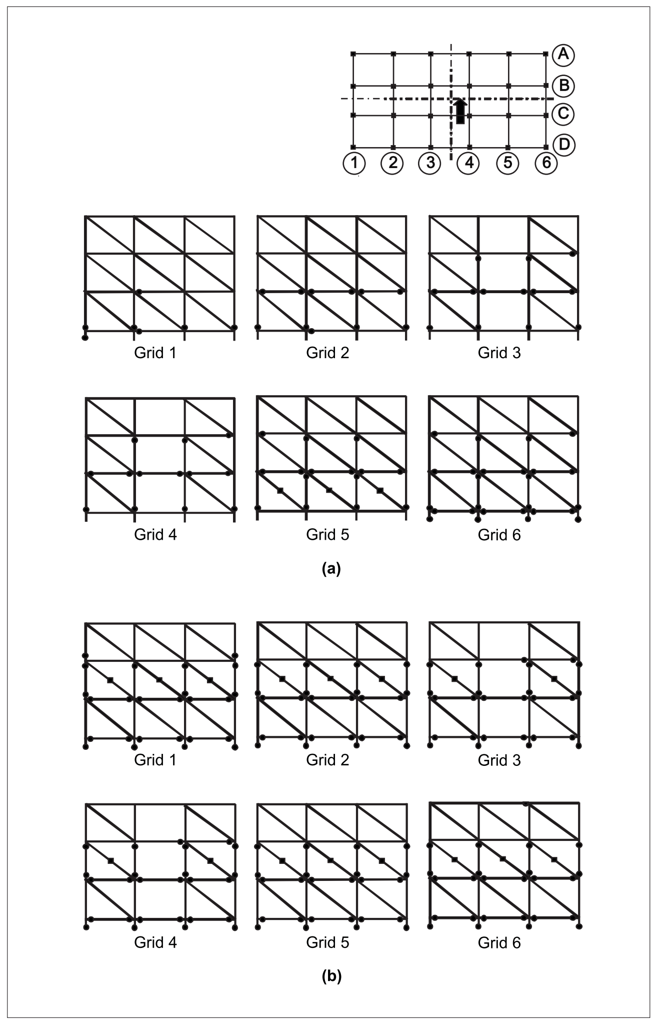

Fig 7 Location of hinges at failure in the infilled building designed as per *(a)* IS: 456 and *(b)* NBC201

case of EBF method the redundancy ratio Ω_r is maximum and it indicates that this building gains the highest post yield strength.

The response reduction factor, *R*, obtained for the infilled frame buildings designed as per IS 456, IS 13920, EC8 and NBC 201 are in a comparable range and higher for the building designed by EBF method. The IS 1893 recommends response reduction factor values of 6.0 and 10.0 for all buildings designed and detailed as per IS 456 and IS 13920 respectively.

The brick infill walls, when present in buildings, are generally observed to bring down the extent of damage. In case of the buildings designed by NBC 201 and EBF method, however, the drift undergone by the bare and infilled structures are comparable. The behaviour of these buildings is also different from that of the others. Therefore, the reduction in the number of plastic hinges formed is not observed in the buildings designed by NBC 201 and the EBF method. In the IS 456 building, yielding initiates simultaneously in both the column and beam members. The other buildings have more desirable responses with the columns yielding after the formation of hinges in different beam members.

It is observed that yielding initiates in the bottom storey members and gradually spreads to the upper storeys at higher displacements, with the top storey members suffering little or no damage, *Fig 7(a)*. The first floor beams yield earlier than the plinth beams. Since the load is applied eccentrically, yielding starts in the members on the right half of the building in plan where the load is applied, *Fig 7(a)*. Due to the strut action of the infill walls, members in the windward side yield earlier.

In the building designed by NBC, the infills are modelled as struts and hence, the demand on the columns above the plinth beam reduces significantly. The building is detailed as per IS:13920 and reinforcements in the columns are same above and below a joint. This resulted in higher strength of the base columns (portion between the plinth beams and the foundations) and the lower half of the ground storey columns. Consequently, with progressive displacements, there is extensive yielding in the columns of the first storey and the beams of the first floor, leading to the formation of a partial storey mechanism, *Fig 7(b)*. Thus, it is evident that plinth beam played a significant role as it resulted in a totally different and unexpected mode of failure.

Concluding remarks

Brick infill walls present in RC frame buildings reduce the structural drift but increase the strength and stiffness. Also, ductility of structures is reduced whereas overstrength is increased due to the presence of infills. The role of the plinth beam is found to be significant when the contribution of infills is taken into account in the building design. Infill walls, when present in a structure, generally bring down the damage suffered by the RC frame members during earthquake shaking. The columns, beams and infill walls of the lower stories are more vulnerable to damage than those in the upper stories.

Of the buildings designed as per the different design procedures, the EBF method of design results in the best utilisation of the beneficial effects of brick masonry infills. The EBF method is useful for design of RC moment resisting frames with unreinforced brick masonry infills to account for increased strength and stiffness due to infills, ensure good seismic behaviour, and take advantage of the presence of infills and provide an economical structural design.

References

1. Saneinejad, A. and Hobbs, B. Inelastic design of infilled frames, *Journal of Structural Engineering,* 1995, *ASCE*, Vol 121, No 4, 634-650.
2. Reinhorn, A.M., Madan, A., Valles, R.E., Reichmann, Y., and Mander, J.B. *Modelling of masonry infill panels for structural analysis*, Technical Report NCEER-95-0018, National Center for Earthquake Engineering Research, Buffalo, 1995.
3. ______CSI *SAP2000: Integrated finite element analysis and design of structures*, Computers and Structures Inc., California, 1999.
4. Das,D. and Murty, C.V.R. Brick masonry infills in seismic design of RC frame buildings : Part 1 – Cost implications, *The Indian Concrete Journal,* July 2004, Vol 78, No 7, pp. 39-44.
5. ______*Seismic evaluation and retrofit of concrete buildings*, ATC 40, Applied Technology Council, California, 1996.
6. Park,R., and Paulay, T. *Reinforced Concrete Structures*, John Wiley and Sons, New York,1975.
7. Dasgupta, P. *Effect of confinement on strength and ductility of large RC hollow sections*, M.Tech. Thesis, Department of Civil Engineering, Indian Institute of Technology Kanpur, 2000.
8. Pillai, E.B.P. *Influence of brick infill on multistorey multibay R.C. frames*, Ph.D. Thesis, Department of civil engineering, Coimbatore Institute of Technology, Coimbatore, 1995.
9. Hatzinikolas, M.A. *Relationship between allowable and ultimate shear stresses in unreinforced brick masonry*, Canadian Masonry Research Institute, Personal Communication, 2000.
10. ______*Indian standard code of practice for structural use of unreinforced masonry*, IS 1905 : 1987, Bureau of Indian Standards, New Delhi, 1987.
11. Das, D. *Beneficial effects of brick masonry infills in seismic design of RC frame buildings,* M.Tech. Thesis, Department of Civil Engineering, Indian Institute of Technology Kanpur, 2000.
12. Raj, G.B.P. *Experimental investigation of RC Frames with brick masonry infill walls having central opening subjected to cyclic displacement loading*, M.Tech. Thesis, Department of Civil Engineering, Indian Institute of Technology Kanpur, India, 2000.
13. ______*Structural engineering design provisions*, UBC 1997, Uniform Building Code, 1997, Vol 2.

Mr Diptesh Das is currently lecturer in the department of applied mechanics and drawing at National Institute of Technology, Durgapur. He received his masters degree from the Indian Institute of Technology Kanpur in 2000. His research interests include earthquake resistant design of RC frame buildings.

Prof C.V.R. Murty is currently associate professor in the department of civil engineering at IIT Kanpur. His areas of interest include research on seismic design of steel and RC structures, development of seismic codes, modelling of nonlinear behaviour of structures and continuing education. He is a member of the Bureau of Indian Standards Sectional Committee on earthquake engineering and the Indian Roads Congress Committee on bridge foundations and substructures, and is closely associated with the comprehensive revision of the building and bridge codes.

● ● ●